Available online at www.sciencedirect.com
SCIENCE DIRECT®
ELSEVIER
Journal of Magnetism and Magnetic Materials 285 (2005) 177–182
Journal of magnetism and magnetic materials
www.elsevier.com/locate/jmmm

In situ TEM study of Nd-rich phase in NdFeB magnet

S.C. Wang[a,b,*], Y. Li[c]

[a] Materials Research Group, School of Engineering Science, The University of Southampton, Southampton SO17 1BJ, UK
[b] Electron Microscopy Centre, Faculty of Engineering and Science, The University of Southampton, UK
[c] School of Metallurgy and Materials, The University of Birmingham, UK

Received 7 June 2004
Available online 13 August 2004

Abstract

Hot stage in transmission electron microscope has been used to study the structure and stability of Nd-rich phase in NdFeB magnet. The present observation shows that the so-called complex cubic phase is in fact the prototype of Mn_2O_3 (space group $Ia\bar{3}$) with lattice parameter of $a = 1.08$ nm. The Nd-rich phase with $P\bar{3}m1$ structure (h-Nd_2O_3) was first observed to be transformed from the BCC phase after in situ heating over 400 °C. The orientation relationship between these two structures satisfies as follows: $(0\,0\,0\,1)_{HCP}//(2\,0\,0)_{BCC}$, $(10\,\bar{1}\,0)_{HCP}//(0\,2\,0)_{BCC}$, $[\bar{1}\,2\,\bar{1}\,0]_{HCP}//[0\,0\,1]_{BCC}$. It is argued that the h-Nd_2O_3 was arising from the oxidation of the BCC Nd-rich phase rather than from $Nd_2Fe_{14}B$ matrix phase as suggested in the literature.

PACS: 75.50.Ww; 61.14.Lj; 68.37.Lp

Keywords: Nd-rich phase; NdFeB magnet; TEM; Amorphous

1. Introduction

The NdFeB magnet normally contains three phases: $Nd_2Fe_{14}B$ matrix, a small volume fraction of $NdFe_4B_4$ phase and Nd-rich phase at grain boundaries [1,2]. Considerable effort has been expended in study of Nd-rich phase since the grain boundary phases are believed to have a strong influence on the coercivity of the magnets.

From the literature, it appears that the Nd-rich regions are rather complex. Four kinds of structures have been reported as shown in Table 1. Fidler [3] observed an Nd-rich phase having a double hexagonal structure (so-called DHCP-Nd_2O_3) in sintered magnets. After annealing at 1080 °C for 50 min, the DHCP phase would transform to an FCC NdO phase (NaCl prototype) [4] at O > 0.57 at% [5]. Under electron irradiation, the

*Corresponding author. Materials Research Group, School of Engineering Science, The University of Southampton, Southampton SO17 1BJ, UK. Tel.: +0044-23-8059-5101; fax: +0044-23-8059-3016.
E-mail address: wangs@soton.ac.uk (S.C. Wang).

0304-8853/$ - see front matter © 2004 Elsevier B.V. All rights reserved.
doi:10.1016/j.jmmm.2004.07.035

Table 1
The crystal structures and lattice parameters of all reported Nd-rich phases

Phase	Prototype	Space group	Lattice parameters, nm	References
DHCP-Nd_2O_3	unknown	HCP	$a = 0.365-0.37$, $c = 1.18$	[3,4]
FCC-NdO	NaCl	$Fm\bar{3}m$	$A = 0.507-0.524$	[4,5]
Complex-Nd_2O_3	unknown	FCC + BCC	$a_{FCC} = 0.52$ and $a_{BCC} = 1.04$	[5,6]
h-Nd_2O_3	La_2O_3	$P\bar{3}m1$	$a = 0.383$, $c = 0.600$	[8]

fundamental FCC patterns of NdO phase were superimposed by weak reflections. Lemarchand et al. [5] and Yin et al. [6] attributed them to a BCC Nd_2O_3 coexistence with an FCC NdO. However, TEM dark field did not favour two phases coexisting, and a BCC superlattice with twice the lattice parameter of the fundamental FCC lattice was suggested [7]. The fourth structure of Nd-rich phases is a HCP structure with the lattice parameters $a = 0.383\,nm$ and $c = 0.600\,nm$ [8], which was proposed arising from the decomposition of matrix phase ($Nd_2Fe_{14}B$) due to the oxidation at high temperatures based on X-ray diffraction (XRD) [9]:

$$Nd_2Fe_{14}B + 3/2O_2 \rightarrow h - Nd_2O_3 + 14Fe + B. \quad (1)$$

This reaction was supported by the recent TEM work on selected area electron diffraction pattern [10]. In contrast, Li et al. [11] found that the product of Nd-rich phase from matrix phase ($Nd_2Fe_{14}B$) was amorphous on high-resolution electron microscopy (HREM).

The purpose of this paper is to clarify the origin of h-Nd_2O_3. Hot stage in TEM was used and the relationship between two Nd-rich structures was first observed.

2. Experimental procedure

The NdFeB magnets used for this study were supplied by Philips Component Ltd. and had a nominal composition of $Nd_{15}Fe_{76.5}B_{7.0}Dy_{0.4}Nb_{0.5}Al_{0.6}$ (at%). The magnets were produced by a powder metallurgy method (ingot → HD → jet milling → powder alignment → pressing → sintering) and were finally demagnetised. The magnets were stuck on a glass slide using a low melting point wax and cut into small pieces about 16 mm in width using a low-speed diamond saw. The pieces were ground on 1200-grid SiC papers to around 80 μm thickness and then glued on a 1×2 mm slot copper grid. The grid was single-side dimpled using 6 μm diamond paste in a South Bay Technology Model 515 dimpler until the thickness at the centre was about 40 μm. Finally, they were ion milled by Gatan DuoMill model 600 using 6 kV voltage and 6–12° Ar ion beam incidence angle until perforation. TEM observations were carried out in a JEOL 4000FX at both room temperature and in situ heating.

3. Results and dicussions

3.1. Nd-rich phase

The microstructure of a sintered magnet consists of matrix grains of approximately 3–7 μm diameter. Fig. 1 shows a triangular region of an Nd-rich phase among $Nd_2Fe_{14}B$ grains. Energy dispersive spectrometer microanalysis indicated the Nd-rich region had 50 ± 10 at% oxygen. Fig. 2(a) shows a series of selected area electron diffraction (SAD) patterns tilted from an Nd-rich phase. These strong and weak diffraction patterns have been suggested to arise from FCC-NdO and BCC-Nd_2O_3 [5,6]. In contrast, TEM work by Chou et al. [7] and by the present authors showed the dark field images were bright in the whole Nd-rich phase, and therefore it ruled out of the possibility of two phases. The whole diffractions in fact satisfy a body-centred cubic structure $Ia\bar{3}$ with the lattice parameter of $a = 1.08\,nm$, and the diffraction patterns of Fig. 2(a) can be indexed

to be [0 0 1], [0 1 1] and [1 1 1], respectively. The simulated diagrams shown in Fig. 2(b), based on coordinates of β-Mn_2O_3 type, correspond well with the real diffraction patterns of Fig. 2(a).

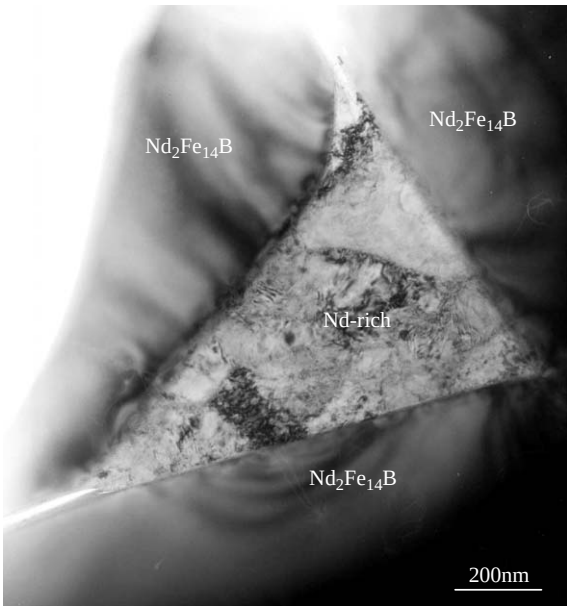

Fig. 1. Bright-field TEM micrograph of the as-received NdFeB magnet, showing $Nd_2Fe_{14}B$ matrix grains and Nd-rich grain boundary phase.

In order to study the stability of the BCC phase, hot stage TEM was performed. Firstly the Nd-rich phase was tilted to [0 0 1] axis (Fig. 3a) at room temperature then was in situ heated in the microscope. It was observed that BCC-Nd_2O_3 was stable up to 300 °C and started to become unstable at 350 °C, and finally transformed to HCP (La_2O_3 prototype) at 400 °C. The orientation relationship between these two structures was determined as following: $(0\,0\,0\,1)_{HCP}//(2\,0\,0)_{BCC}$, $(1\,0\,\bar{1}\,0)_{HCP}//(0\,2\,0)_{BCC}$, $[\bar{1}\,2\,\bar{1}\,0]_{HCP}//[0\,0\,1]_{BCC}$.

3.2. $Nd_2Fe_{14}B$ phase

The matrix $Nd_2Fe_{14}B$ phase was also observed to decompose during the in situ heating. Fig. 4(a) shows $[1\,2\,1]_{Nd_2Fe_{14}B}$ zone of as-received sample. After continuous heating inside the microscopy, diffraction rings of polycrystalline α-Fe appear to superimpose on the diffraction pattern of the $Nd_2Fe_{14}B$ phase after 300 °C as shown in Fig. 4(b). At 400 °C the diffraction spots of the $Nd_2Fe_{14}B$ phase completely disappear, as shown in Fig. 4(c). To study the origin of diffraction rings, the theoretical spacings of α-Fe (Table 2) have been ringed to compare the observed diffraction rings (Fig. 4c). As shown in Fig. 5, the spacings of α-Fe crystallines, designated by solid lines, match all the observed diffraction

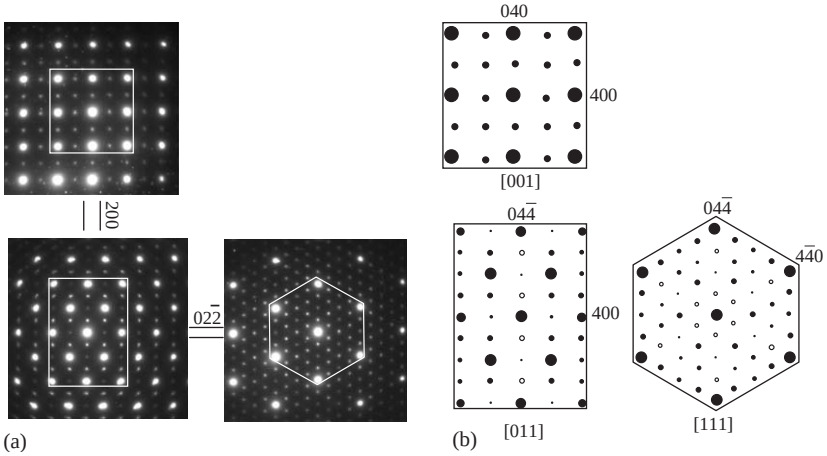

Fig. 2. (a) A series of SAD patterns tilted from one Nd-rich phase in the as-received sample; (b) Simulated diffraction patterns for Nd-rich phase based on the $Ia\bar{3}$ structure (Mn_2O_3 type) with lattice parameter $a = 1.08$ nm. The solid and open circles represent real and double diffractions, respectively.

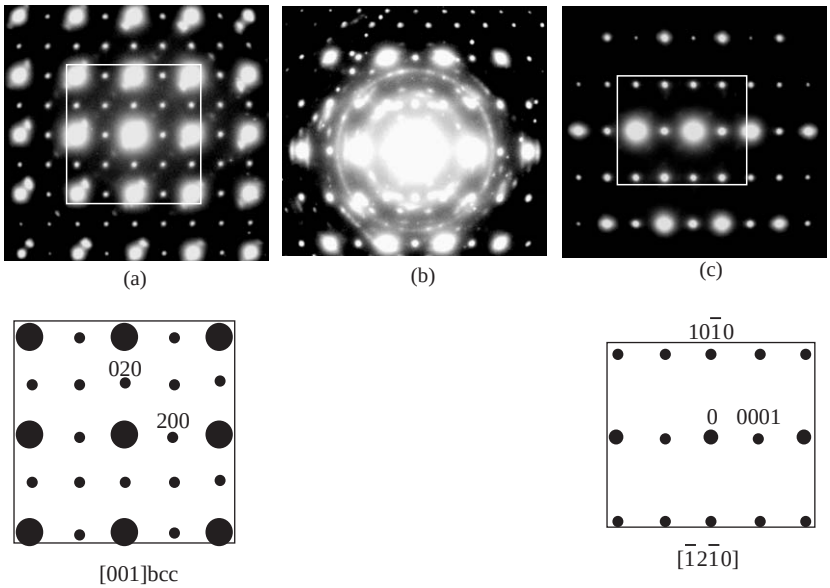

Fig. 3. SAD patterns from Nd-rich phase in hot stage TEM, showing structure changing from [0 0 1] of $Ia\bar{3}$ to $[\bar{1}\,2\,\bar{1}\,0]$ of $P\bar{3}m1$. (a) $[0\,0\,1]_{BCC}$ at room temperature; (b) 350 °C; (c) $[\bar{1}\,2\,\bar{1}\,0]_{HCP}$ at 400 °C.

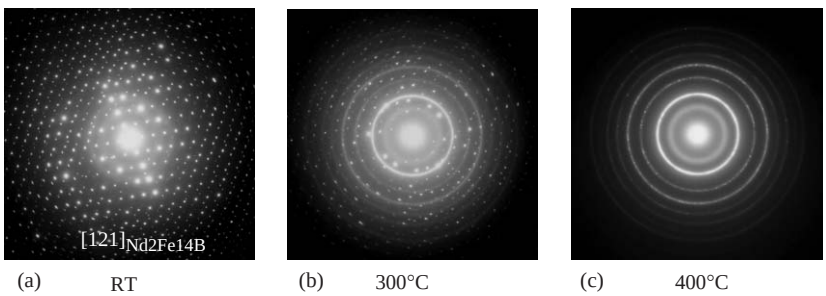

Fig. 4. SAD patterns from $Nd_2Fe_{14}B$ phase in a hot stage in a TEM, showing the dissociation process of the $Nd_2Fe_{14}B$ phase by oxidation. (a) Room temperature; (b) 300 °C; and (c) 400 °C.

rings, except a broad diffraction ring with a mean spacing of $d = 0.3$ nm (designated as I in Fig. 5). Furthermore, the diffraction intensities of α-Fe, shown in Table 2, are consistent to the intensities of the observed diffractions (as shown in Fig. 5). The broad ring of the spacing of 0.3 nm, which cannot be explained by the structure of α-Fe, was attributed to h-Nd_2O_3 by Zhu et al. [10]. However, most of spacings of h-Nd_2O_3, as drawn by dashed semi-cycles in Fig. 5 do not match the actual diffraction rings. Interestingly, the SAD on amorphous Nd-rich phase [12] showed a diffusion ring of the same spacing (0.3 nm). Therefore, the diffusion ring I in Fig. 5 is more appropriate from the amorphous regions rather than from the crystallines of h-Nd_2O_3. This argument has been further supported by HREM. Fig. 6 shows a high-resolution micrograph from a sample after oxidation at 400 °C for 2 days. The spacing of 0.20 nm, which corresponding to 1 1 0 planes of α-Fe, can be dissolved clearly. And amorphous regions around 2 nm in diameter

Table 2
X-ray diffraction densities of h-Nd_2O_3 and α-Fe

Spacing (nm)	h-Nd_2O_3		α-Fe	
	h k l	Intensity	*h k l*	Intensity
0.3317	100	30		
0.2999	002	28		
0.2903	011	100		
0.2225	012	25		
0.2027			110	100
0.1915	110	29		
0.1443			200	20
0.1170			211	30
0.1013			220	10
0.9064			310	12

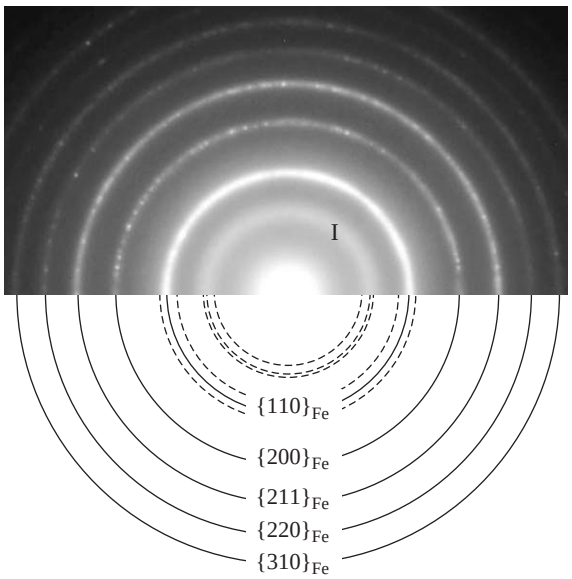

Fig. 5. Upper half showing the enlargement of Fig. 4c and lower half showing indexed planes of α-Fe and h-Nd_2O_3. The solid and dashed semi-circles represent the diffractions from α-Fe and h-Nd_2O_3.

(some regions are circled) are dispersed among these α-Fe crystallines.

4. Conclusions

The present observation shows that complex-Nd_2O_3 has the prototype of Mn_2O_3 (space group

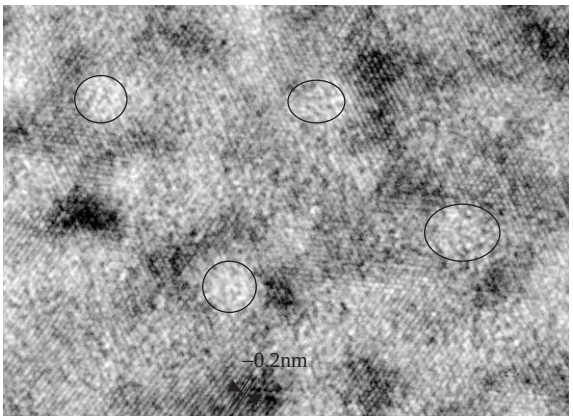

Fig. 6. High-resolution TEM micrograph after oxidation at 400 °C for 2 days, showing amorphous Nd-oxide regions (some are circled) embedded in α-Fe matrix.

$Ia\bar{3}$) with lattice parameter of $a = 1.08$ nm. The BCC phase will further oxidise to $P\bar{3}m1$ structure (prototype of La_2O_3). Diffraction and HREM support the argument that h-Nd_2O_3 forms from complex-Nd_2O_3 rather than from the decomposition of the $Nd_2Fe_{14}B$ matrix.

Acknowledgment

The paper is part of Ph.D. work (Y. Li) and Y. Li would like to thank professors I.R. Harris and I.P. Jones of Birmingham University, UK and Professor M. Aindow of University of Connecticut, USA for the Ph.D. supervision. Financial support was provided by the committee of Vice Chancellors and Principals under the Oversea Research Scholar (ORS) Scheme, School of Metallurgy and Materials, The University of Birmingham and School of Engineering Science, The University of Southampton.

References

[1] D. Givord, J.M. Moreau, P. Tenaud, Solid State Commun 55 (1985) 303.
[2] N.F. Chaban, Y.B. Kuzma, N.S. Bolinizhko, O. Kachmar, N.U. Petrov, Dopov. Akad. Nauk SSSR, Ser. A. 10 (1979) 873.

[3] J. Fidler, IEEE Trans. Magn. 21 (1985) 1955.
[4] W. Tang, S. Zhou, R. Wang, J. Less-Common Metals 14 (1988) 217.
[5] D. Lemarchand, P. Vigier, B. Labulle, IEEE Trans. Magn. 26 (1990) 2649.
[6] X.Y. Jin, I.P. Jones, I.R. Harris, J. Magn. Magn. Mater. 125 (1993) 91.
[7] T.Y. Chu, L.K. Rabenburg, Proceeding of the XII International Congress for Electron Microscopy, 1990, p. 994.
[8] D. Grier, G. McCarthy, North Dakota State University, Fargo, North Dakota, USA. ICDD Grant-in-Aid 1991.
[9] D.S. Edgley, J.M. Breton, S. Steyaert, F.M. Ahmed, I.R. Harris, J. Teillet, J. Magn. Magn. Mater. 173 (1997) 29.
[10] L.Y. Zhu, M. Itakura, Y. Tomokiyo, N. Kuwano, K. Machida, J. Magn. Magn. Mater. 279 (2004) 353.
[11] Y. Li, H.E. Evan, I.R. Harris, I.P. Jones, Oxidation of Metals 39 (2003) 167.
[12] J. Holc, S. Besenicar, D. Kolar, J. Mater. Sci. Lett. 25 (1990) 215.